Supporting Information

Long-term degradation mechanisms in application-implemented radical thin films

*Ewa Malgorzata Nowik-Boltyk,[†] Tobias Junghoefer,[†] Mathias Glaser,[†] Erika Giangrisostomi,[#] Ruslan Ovsyannikov,[#] Shuyang Zhang,[§] Chan Shu,[§] Andrzej Rajca,[§] Arrigo Calzolari,[‡] M. Benedetta Casu[†]**

[†]*Institute of Physical and Theoretical Chemistry, University of Tübingen, 72076 Tübingen, Germany*

[#]*Institute Methods and Instrumentation for Synchrotron Radiation Research, Helmholtz-Zentrum Berlin, 12489 Berlin, Germany*

[§]*Department of Chemistry, University of Nebraska, Lincoln, NE 68588, United States*

[‡]*CNR-NANO Istituto Nanoscienze, Centro S3, 41125 Modena, Italy*

Corresponding Author

*E-mail: benedetta.casu@uni-tuebingen.de, Tel. +49 7071 29 76252, Fax: +49 7071 29 5490 (M.B.C.).

Table of contents

1) Fit parameters for the freshly evaporated Blatter-pyr films as in Figure 1. The fit has been performed as described in references [1-5].

The expected stoichiometric values for the C 1s and N 1s elemental analyses are:

C-C = 24%, C-H = 62%, C-N = 14%, and $N_{radical} = N_{imino} = N_{amino} = 33\%$

Table S1

	Energy (eV)	Lorentzian Width (eV)	Gaussian Width (eV)	Intensity (%)
C-C	284.4	0.08	0.90	17.7
C-H	284.8	0.08	0.90	47.9
S_1	285.4	0.08	0.90	1.2
C-N	285.9	0.08	0.90	11.6
S_2	286.6	0.08	0.90	4.3
S_3	287.5	0.08	0.90	1.1
S_4	288.4	0.08	1.44	2.0
S_5	291.6	0.08	5.14	14.2

C-C + S_1+S_3+S_4=22.0%, C-H+ S_5=62.1%, C-N + S_2=15.9%

Table S2

	Energy (eV)	Lorentzian Width (eV)	Gaussian Width (eV)	Intensity (%)
N_{rad}	398.3	0.1	0.8	28.6
N_2	399.2	0.1	0.8	28.1
S_1	400.1	0.1	0.8	5.2
N_1	401.0	0.1	0.8	29.7
S_2	402.1	0.1	0.8	6.1
S_3	403.0	0.1	0.8	2.3

$N_{rad}+S_1$= 33.8%, N_2+S_2= 34.2 %, N_1+S_3=32.0%

Fit parameters for the freshly evaporated diBlatter films as in Figure 2.

The expected stoichiometric values for the C 1s and N 1s elemental analyses are:

C-C = 11.1%, C-H = 66.7%, C-N = 22.2%, and $N_{radical} = N_1 = N_2 = 33\%$

Table S3

	Energy (eV)	**Lorentzian Width (eV)**	**Gaussian Width (eV)**	**Intensity (%)**
C-C	284,9	0.08	1.0	11.9
C-H	285,3	0.08	1.0	52.7
S_1	285,9	0.08	1.0	1.6
C-N	286,3	0.08	1.0	19.9
S_2	287,0	0.08	1.0	8.8
S_3	287,7	0.08	1.5	1.8
S_4	292,2	0.08	3.1	3.3

C-C + S_1 =13.5%, C-H+½ S_2+S_3+S_4=62.2%, C-N + ½ S_2=24.3%

Table S4

	Energy (ev)	Lorentzian Width (eV)	Gaussian Width (eV)	Intensity (%)
N_{rad}	398.9	0.1	0.95	26.1
$N_{1,3}$	399.9	0.1	0.95	28.5
$N_{2,4}$	401.7	0.1	0.95	29.9
S_1	400.6	0.1	0.95	5.9
S_2	402.2	0.1	0.95	3.0
S_3	402.4	0.1	0.95	3.0
S_4	403.3	0.1	0.95	2.1
S_5	404.3	0.1	0.95	1.5

$N_{rad} + ½(S_1 + S_2) + S_4 + S_5 = 34.1$ %
$N_{1/3} + ½(S_1 + S_2) = 33.0$ %
$N_{2/4} + S_3 = 32.9$ %

2) Time dependent core level signals.

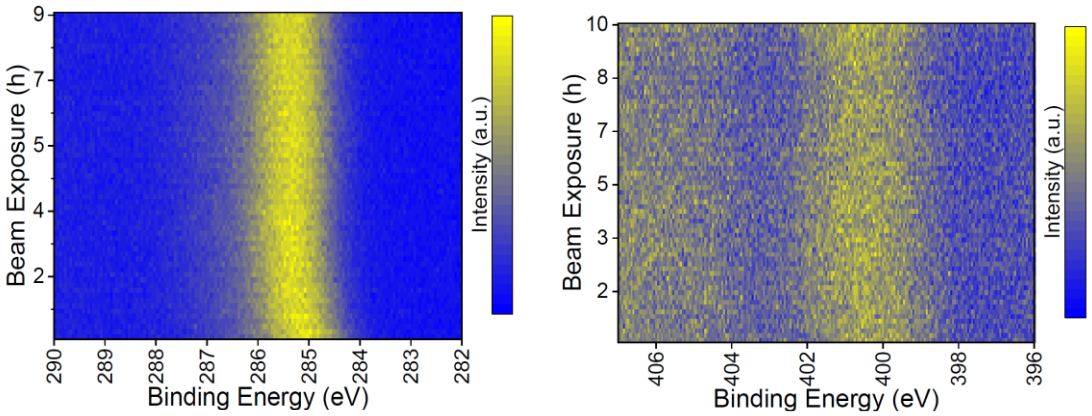

Figure S1. diBlatter thin films. (Left) Time-dependent C 1s and (right) N 1s core level signals. Color scale: Blue represents the background signal; yellow is the peak intensity (photon energy: 700 eV).

3) Time-dependent NEXAFS signals.

The unoccupied states and the molecular arrangement adopted by the molecules in the thin films can be investigated by NEXAFS spectroscopy. NEXAFS features and their intensities are sensitive to intermolecular interactions, and NEXAFS dichroism allows determining the orientation of the molecules with respect to the substrate.[6, 7] In particular, the main resonance at around 286.0 eV can be identified as due to the pyrene substituent, leading to a calculated average orientation of the pyrene plane of 30°. The observed dichroic behavior is the typically dichroic expected one for the herringbone structure,[8-10] due to the compromise between the strength of the C-H and the π–π interactions.[11]

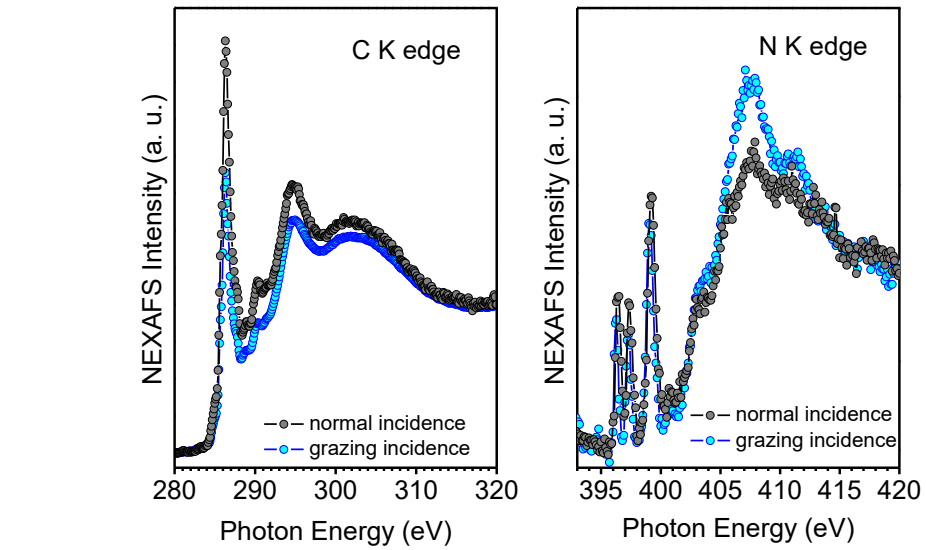

a) b)

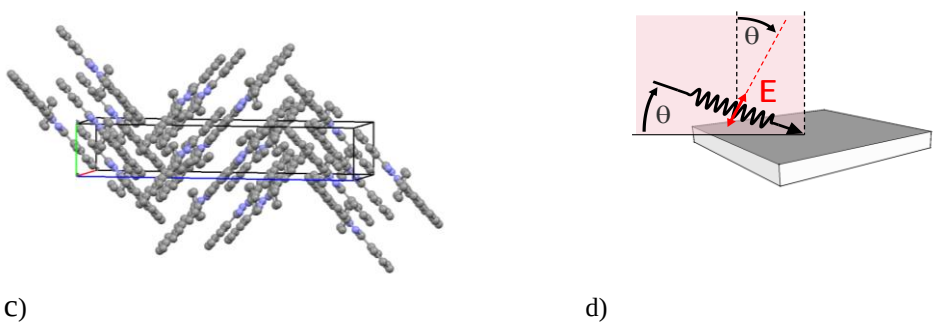

c) d)

Figure S2. Blatter-pyr. a) C K edge and b) N K edge NEXAFS spectra of a nominally 3.5 nm thick film. c) Crystal structure. d) Geometry of the experiment.

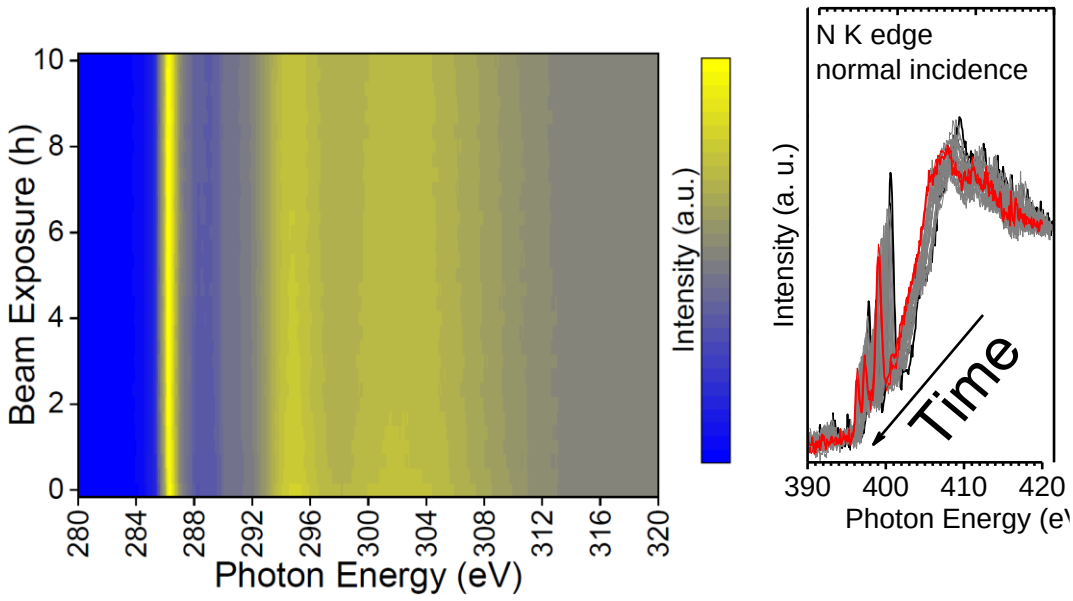

Figure S3. Blatter-pyr thin films. NEXAFS intensity versus beam exposure.

4) C 1s core level spectra after air exposure.

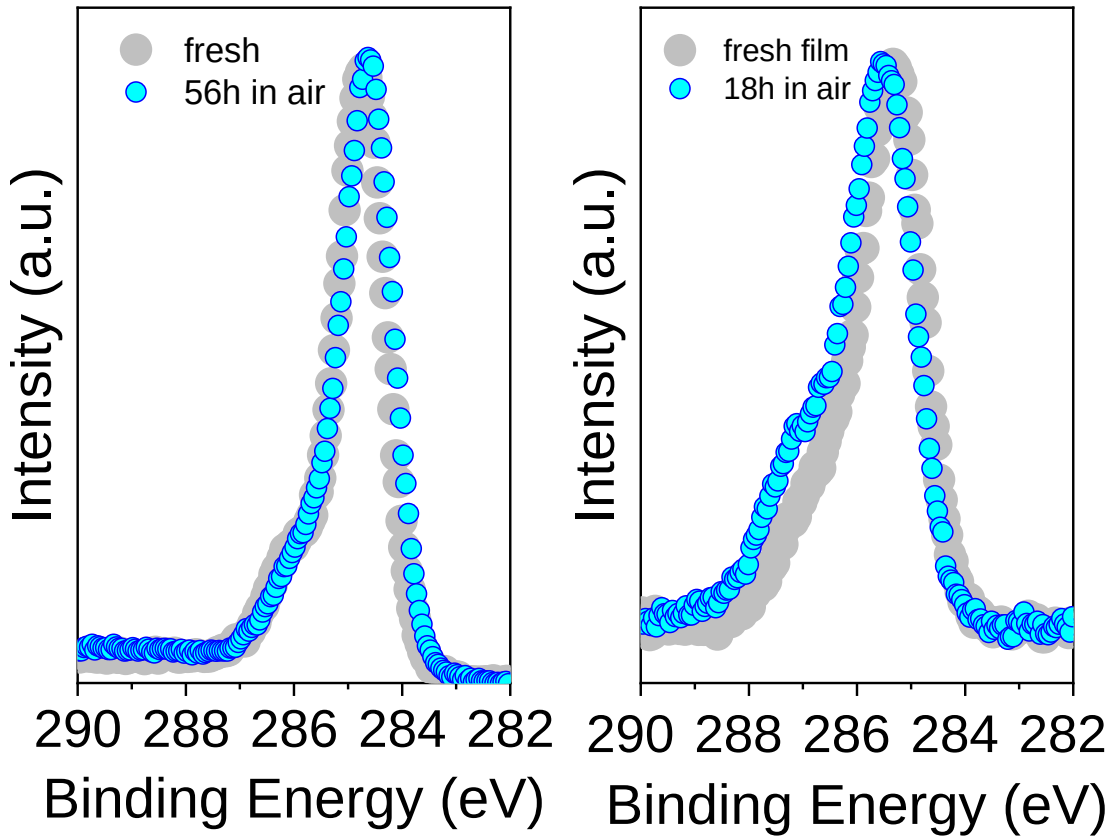

a) b)

Figure S4. C 1s core level spectra of a) Blatter-pyr and b) diBlatter thin films, after air exposure, as indicated. The fresh film core level curves (light grey) are also shown for comparison (photon energy: 1486.6 eV).

5) Fit parameters for Blatter-pyr films as in Figure 3 after 45 hours of air exposure

Table S5

	Energy (eV)	Lorentzian Width (eV)	Gaussian Width (eV)	Intensity (%)
C-C	284.4	0.08	0.90	23.9
C-H	284.8	0.08	0.90	41.0
S_1	285.6	0.08	0.90	2.3
C-N	285.8	0.08	0.90	10.1
S_2	286.6	0.08	0.90	3.8
S_3	287.5	0.08	0.90	0.5
S_4	288.3	0.08	2.45	4.4
S_5	291.6	0.08	5.14	14.0

Table S6

	Energy (eV)	Lorentzian Width (eV)	Gaussian Width (eV)	Intensity (%)
N_{rad}	398.3	0.1	0.8	27.0
N_2	399.2	0.1	0.8	28.6
S_1	400.1	0.1	0.8	6.4
N_1	401.0	0.1	0.8	29.1
S_2	402.0	0.1	0.8	5.8
S_3	403.0	0.1	0.8	3.1

Fit parameters for diBlatter films as in Figure 3 after 72 hours of air exposure.

Table S7

	Energy (eV)	Lorentzian Width (eV)	Gaussian Width (eV)	Intensity (%)
C-C	284.9	0.08	1.0	11.2
C-H	285.4	0.08	1.0	55.9
S_1	285.9	0.08	1.0	1.7
C-N	286.3	0.08	1.0	17.9
S_2	287.0	0.08	1.0	7.7
S_3	287.7	0.08	1.3	2.8
S_4	292.2	0.08	3.8	2.8

Table S8

	Energy (eV)	Lorentzian Width (eV)	Gaussian Width (eV)	Intensity (%)
N_{rad}	398.9	0.1	0.95	16.3
$N_{1,3}$	399.9	0.1	0.95	28.6
N*	400.8	0.1	0.95	25.0
$N_{2,4}$	401.7	0.1	0.95	20.4
S_2	402.2	0.1	0.95	1.3
S_3	402.4	0.1	0.95	4.3
S_4	403.4	0.1	0.95	2.5
S_5	404.3	0.1	0.95	1.6

6) Spin-polarized density of states of the Blatter-pyr.

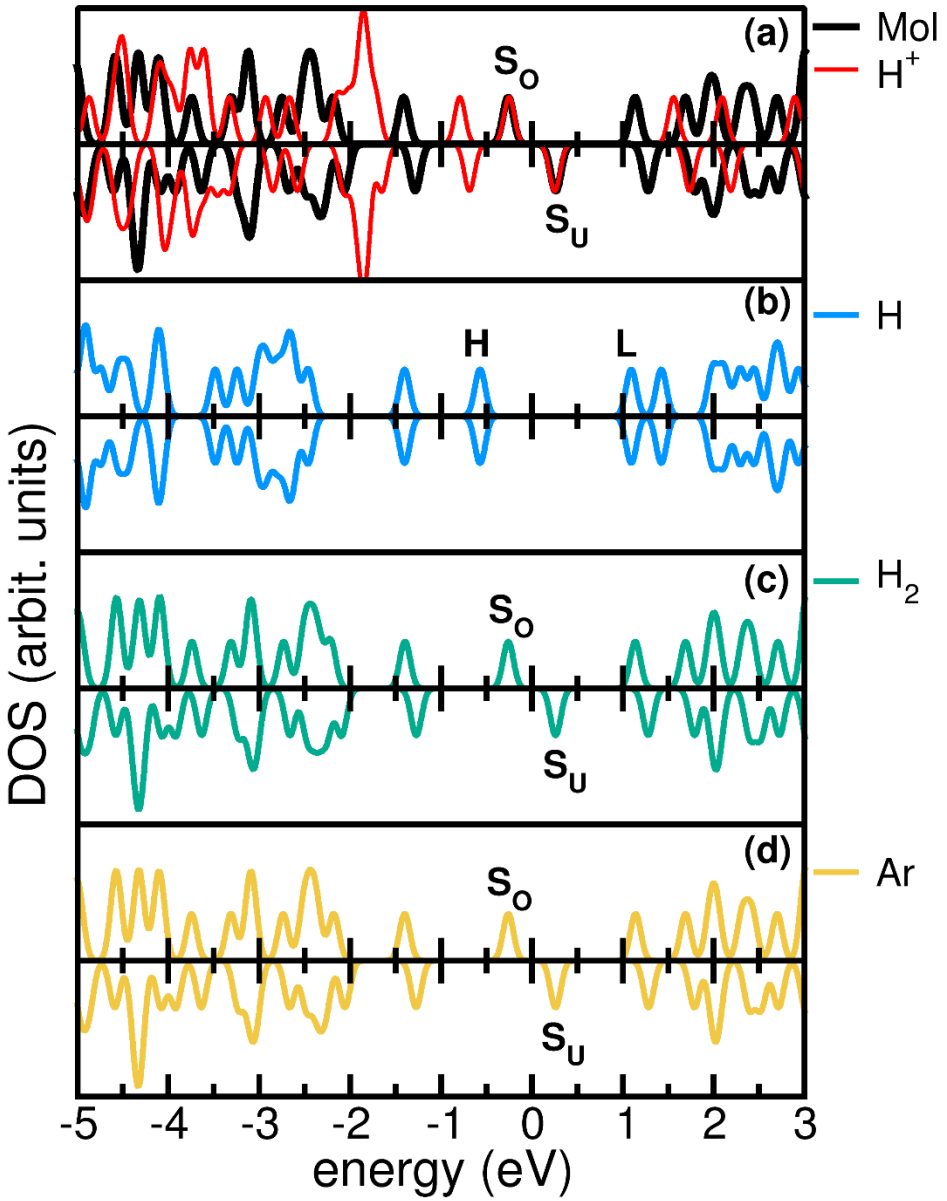

Figure S5. Spin-polarized density of states (DOS) of the Blatter-pyr without (black line, panel a) and with selected adsorbed impurities: H^+ (red line, panel a), H (cyan line, panel b), H_2 (green line panel c), and Ar (yellow line, panel d). Negative/positive energies indicate occupied/empty electronic states: highest Single Occupied (S_O) and lowest Single Unoccupied (S_U) molecular orbitals are indicated (panels a,c,d) , along with double occupied HOMO (H) and LUMO (L) states (panel b). All elements/molecules are adsorbed on site S1.

7) Spin-polarized density of states (DOS) of the diBlatter.

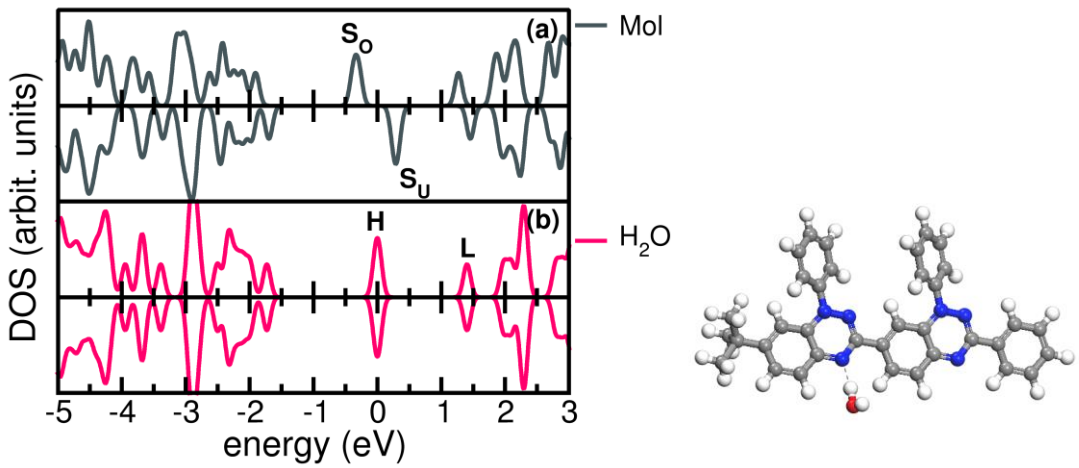

Figure S6. Spin-polarized density of states (DOS) of diBlatter radical (black line, panel a) and of the same molecule with H_2O molecule adsorbed in site S1' (pink line, panel b). Negative/positive energies indicate occupied/empty electronic states: double degenerate highest Single Occupied (S_O) and lowest Single Unoccupied (S_U) molecular orbitals are indicated (panels a), along with double degenerate/double occupied HOMO (H) and LUMO (L) states (panel b). Relaxed geometry upon water molecule adsorption is shown on right.

8) Simulated N 1s core level spectra of Blatter-pyr upon adsorption of characteristic H^+, H_2, Ar, and OH species and as a function of the adsorption sites (S1).

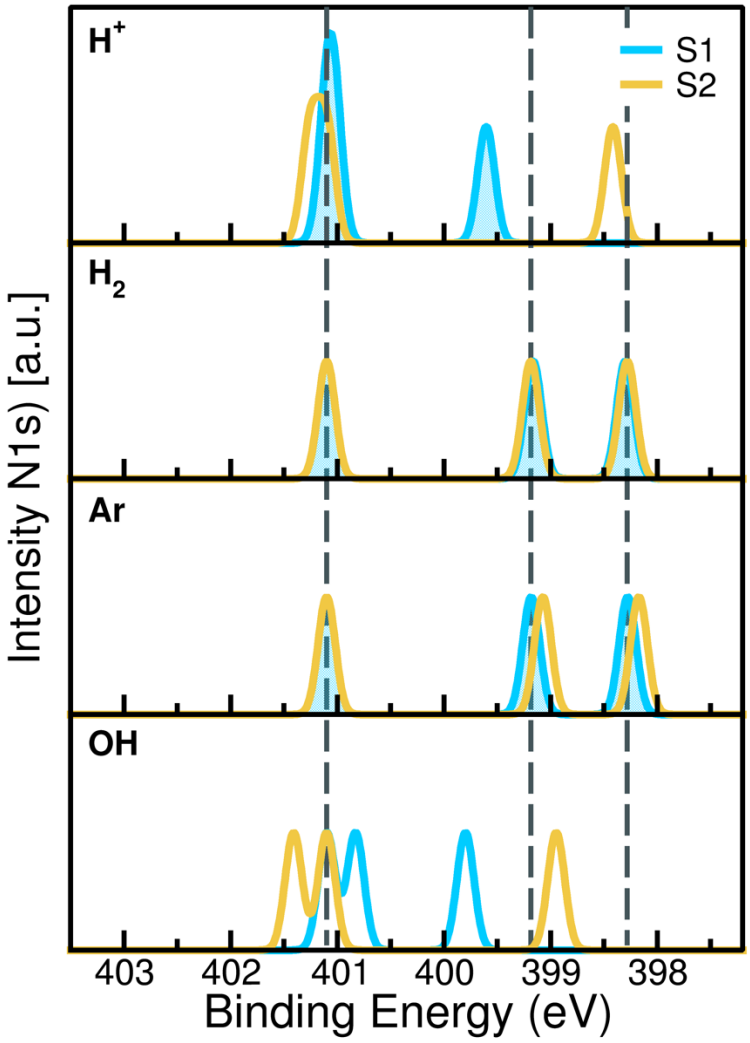

Figure S7. Simulated N 1s core level spectra of Blatter-pyr upon adsorption of characteristic H^+, H_2, Ar, and OH species and as a function of the adsorption sites (S1). Vertical dashed lines refer to the core-level features of the pristine molecules. The N_3 peak is assumed as the energy reference for all spectra and aligned to the experimental value for a direct comparison. Labels and colors refer to Figure 5, main text.

9) References

1. S. Zhang, M. Pink, T. Junghoefer, W. Zhao, S.-N. Hsu, S. Rajca, A. Calzolari, B. W. Boudouris, M. B. Casu and A. Rajca, *J. Am. Chem. Soc.*, 2022, **144**, 6059-6070.
2. T. Junghoefer, E. M. Nowik-Boltyk, J. A. de Sousa, E. Giangrisostomi, R. Ovsyannikov, T. Chassé, J. Veciana, M. Mas-Torrent, C. Rovira, N. Crivillers and M. B. Casu, *Chem. Sci.*, 2020, **11**, 9162-9172.
3. F. Ciccullo, N. M. Gallagher, O. Geladari, T. Chasse, A. Rajca and M. B. Casu, *ACS Appl. Mater. Interfaces*, 2016, **8**, 1805–1812.
4. S.-A. Savu, I. Biswas, L. Sorace, M. Mannini, D. Rovai, A. Caneschi, T. Chassé and M. B. Casu, *Chem.-Eur. J.* , 2013, **19**, 3445-3450.
5. S.-A. Savu, M. B. Casu, S. Schundelmeier, S. Abb, C. Tonshoff, H. F. Bettinger and T. Chassé, *RSC Adv.*, 2012, **2**, 5112-5118.
6. J. Stöhr, *NEXAFS Spectroscopy*, Springer, 2003.
7. J. Stöhr, K. Baberschke, R. Jaeger, R. Treichler and S. Brennan, *Phys. Rev. Lett.*, 1981, **47**, 381-384.
8. T. Breuer, M. Klues and G. Witte, *Journal of Electron Spectroscopy and Related Phenomena*, 2015, **204**, 102-115.
9. M. B. Casu, B.-E. Schuster, I. Biswas, C. Raisch, H. Marchetto, T. Schmidt and T. Chassé, *Adv. Mater.*, 2010, **22**, 3740-3744.
10. S.-A. Savu, A. Sonström, R. Bula, H. F. Bettinger, T. Chassé and M. B. Casu, *ACS Appl. Mater. Interfaces*, 2015, **7**, 19774-19780.
11. C. C. Mattheus, G. A. de Wijs, R. A. de Groot and T. T. M. Palstra, *J. Am. Chem. Soc.*, 2003, **125**, 6323-6330.